Curcumin inhibits prostate cancer metastasis *in vivo* by targeting the inflammatory cytokines CXCL1 and -2

Peter H.Killian[1], Emanuel Kronski[1], Katharina M. Michalik[1], Ottavia Barbieri[2,3], Simonetta Astigiano[2], Christian P.Sommerhoff[1], Ulrich Pfeffer[4], Andreas G.Nerlich[5] and Beatrice E.Bachmeier,[1,4,*]

[1]Institute of Laboratory Medicine (former Dept. of Clin. Chemistry and Biochemistry), Ludwig-Maximilians-University, Munich, Germany [2]IRCCS AOU San Martino-IST National Cancer Research Institute, Genoa, Italy, [3]Department of Experimental Medicine, University of Genoa, Genoa, Italy, [4]Integrated Molecular Pathology, University Hospital San Martino – National Cancer Research Institute, Genoa, Italy and [5]Institute of Pathology, Academic Hospital Munich-Bogenhausen, Munich, Germany

*To whom correspondence should be addressed. Tel: +49-89-5160-2543; Fax: +49-89-5160-4735;
Email: bachmeier.beatrice@gmail.com

In America and Western Europe, prostate cancer is the second leading cause of death in men. Emerging evidence suggests that chronic inflammation is a major risk factor for the development and metastatic progression of prostate cancer. We previously reported that the chemopreventive polyphenol curcumin inhibits the expression of the proinflammatory cytokines CXCL1 and -2 leading to diminished formation of breast cancer metastases. In this study, we analyze the effects of curcumin on prostate carcinoma growth, apoptosis and metastasis. We show that curcumin inhibits translocation of NFκB to the nucleus through the inhibition of the IκB-kinase (IKKβ, leading to stabilization of the inhibitor of NFκB, IκBα, in PC-3 prostate carcinoma cells. Inhibition of NFκB activity reduces expression of CXCL1 and -2 and abolishes the autocrine/paracrine loop that links the two chemokines to NFκB. The combination of curcumin with the synthetic IKKβ inhibitor, SC-541, shows no additive or synergistic effects indicating that the two compounds share the target. Treatment of the cells with curcumin and siRNA-based knockdown of CXCL1 and -2 induce apoptosis, inhibit proliferation and downregulate several important metastasis-promoting factors like COX2, SPARC and EFEMP. In an orthotopic mouse model of hematogenous metastasis, treatment with curcumin inhibits statistically significantly formation of lung metastases. In conclusion, chronic inflammation can induce a metastasis prone phenotype in prostate cancer cells by maintaining a positive proinflammatory and prometastatic feedback loop between NFκB and CXCL1/-2. Curcumin disrupts this feedback loop by the inhibition of NFκB signaling leading to reduced metastasis formation *in vivo*.

Introduction

Curcumin (diferuloylmethane; (1E,6E)-1,7-bis (4-hydroxy-3-methoxyphenyl)-1,6-heptadiene-3,5-dione) is a polyphenol that naturally occurs in the zingiberaceae *Curcuma longa* and is used as turmeric, the main ingredient of curry. It is also used as a food additive, E100, for its strong yellow color.

In the last 20 years, many studies have addressed pharmacological activities of curcumin and especially its anticancer activities are now well established (1). Its antitumoral activities have been observed for many cancers including colon (2), breast (3), head and neck (4), lung (5) and prostate (6) cancer. However, protumoral activities have also been observed (7).

Abbreviations: ANOVA, analysis of variance; DAPI, 4′,6-diamidino-2-phenylindole; EFEMP, EGF-containing fibulin-like extracellular matrix protein; IKK, inhibitor of kappaB kinase; NFκB, nuclear factor kappa B; PBS, phosphate-buffered saline; siRNA, small interfering RNA.

The anticancer activities are apparently mainly mediated by its inhibitory effect on the transcription factor complex, nuclear factor kappa B (NFκB) (8), that plays a central role in inflammation and (anti-) apoptosis and radio- and chemoresistance. Inhibition of NFκB is achieved by curcumin through the inhibition of IKK (inhibitor of kappaB kinase (9,10)) either directly (10) or through the action on upstream activators of IKK (9). Inflammation is considered as a major factor for tumor progression (11), and inhibition of NFκB activation and translocation is a common theme in cancer chemoprevention (12). Antiapoptosis appears to be an important mechanism of resistance to chemotherapy that might be controlled by the inhibition of NFκB (13) and, indeed, curcumin shows such activity (14,15).

Curcumin has also been reported to affect other signaling pathways such as src/Akt (16), c-jun/AP1 (17), protein kinase C (18), sonic hedgehog (19) and others(1). Its activity as a low-affinity ligand of the estrogen receptor has also been proposed (20).

Curcumin is a lipophilic compound and intestinal resorption is low. Free curcumin is detected in plasma at low levels (21). Curcumin is reduced to di- and tetrahydrocurcumin by intestinal *Escherichia coli* (22). Major metabolites are glucuronide conjugates (23). Exposure to the polyphenol is direct for cancers of the gastrointestinal tract but despite its reduced bioavailability, the effects of curcumin on the progression of other solid tumors are well documented. We have recently reported a significant effect on the formation of breast cancer metastases in a murine model of hematogenous metastasis where curcumin reduced the number of lung metastases (3) through the downregulation of NFκB-dependent expression of chemokines (24).

These data point at an application of curcumin for the prevention of cancer progression. Given its anticancer and antiinflammatory activities, curcumin becomes a natural candidate for the prevention of inflammation-related cancers. Moreover, prevention is particularly interesting for clinical situations in which a low-risk tumor is not necessarily excised immediately upon diagnosis. These two features apply to prostate cancer because inflammation plays an important role in its etiology and progression (25) and 'watchful waiting' is an option for selected groups of elderly patients (26). In addition, benign prostate hyperplasia, a condition that can develop into cancer, is also linked to inflammation (27) with cyclooxygenase-2, PTGS2/COX2, being a central mediator (28). COX2 is among the NFκB targets that are downregulated by curcumin in breast cancer cells (24).

We, therefore, wished to establish whether curcumin can inhibit prostate cancer progression to metastasis. We analyzed the effects of the polyphenol on the highly aggressive PC-3 prostate cancer cells in a murine model of hematogenous metastasis and identified the molecular mediators of the significant antimetastatic effect observed.

Materials and methods

Cell types and culture conditions

The human prostate cancer cell line PC-3 used in this study was obtained from the American Type Tissue Culture Collection (Rockville, MD). The cell line is androgen receptor insensitive and was initiated from a bone metastasis of a grade IV prostatic adenocarcinoma from a 62-year-old male Caucasian (29).

The cell line is commonly used for prostate cancer studies and is well defined in its growth, invasive and metastatic characteristics.

The cell line was cultured at 37°C in a humidified atmosphere of 5% CO_2. The cells were grown in RPMI medium (PAN, Aidenbach, Germany) supplemented with 5% heat inactivated fetal calf serum (PAA, Pasching, Austria), 1% L-glutamine solution (200 mM) (PAN, Aidenbach, Germany), 1% sodium pyruvate solution (100 mM) (PAN, Aidenbach, Germany), non-essential amino acids and vitamins (PAN, Aidenbach, Germany). Medium was changed every 2 days.

Curcumin treatment of cells

Curcumin with a purity of 95% was purchased from Fluka (Buchs, Switzerland), dissolved in 0.5 M NaOH as a 25 mM stock solution and stored at –20°C. For the use in cell culture a 2.5 mM solution in sterile phosphate-buffered saline (PBS) was prepared. According to the IC_{50} value of PC-3 cells determined by us previously, curcumin was applied at an end concentration of 15 µM for all assays. For controls, the carrier (0.5 M NaOH) diluted accordingly to the curcumin working solutions in PBS was applied to the cells.

Gene silencing

RNA interference was used to generate specific knockdowns of p65 (NFκB), IκBα, CXCL1 and -2 mRNA transcripts in the human prostate cancer cell line PC-3. Small interfering RNAs (siRNAs) [r(GAUCAAUGGCUACACAGGA) d(TT) and r(UCCUGUGUAGCCAUUGAUC) d(TT)] targeted to NFκB were synthesized and annealed (Qiagen, Hilden, Germany). Predesigned annealed double-stranded siRNAs targeted to IκBα, CXCL1, CXCL2 and CXCR2 were synthesized and purchased by Ambion (Applied Biosystems, Darmstadt, Germany). A non-silencing fluorescein labeled siRNA (Qiagen) was used as control for transfection efficiency and for monitoring the effect of silencing during all experiments. Cell cultures with at least 90% transfection efficiency were used for further studies. Transfection of PC-3 cells (40% confluency) with siRNA was performed using Lipofectamine 2000 (Invitrogen, Carlsbad, CA) according to the recommendations of the manufacturer. Briefly, the transfection reagent was preincubated with the siRNA oligos either targeted to NFκB, IκBα, CXCL1, -2 and CXCR2 or to an irrelevant control 30 min prior to the application to the cells.

Preparation of conditioned media

Cell culture supernatants of curcumin- and mock-treated PC-3 cells were collected and centrifuged 15 min at 4000*g* in order to remove dead cells. The supernatants were used for western blots.

Preparation of cellular extracts

Cells were washed three times with PBS and collected by scraping and centrifuging. Lysis buffer (10 mM Na_3PO_4, 0.4 M NaCl and 0.2% Triton X-100) supplemented with 1 mM phenylmethylsulfonyl fluoride (Fluka, Buchs, Switzerland) and a protease inhibitor cocktail (Sigma–Aldrich, St Louis) was added to the pellets and the mixture was sonicated. After centrifugation for 15 min at 15 000*g*, the supernatant containing the soluble proteins was collected and either analyzed immediately or stored at –80°C.

Determination of protein concentration

Protein concentrations were determined by the bicinchoninic acid protein assay (Pierce, Oud-Beijerland, Netherlands) with bovine serum albumin as standard.

Preparation of RNA and cDNA

Total RNAs were isolated from cells using the RNeasy Mini Kit (Qiagen, Hilden, Germany) according to the manufacturer's instructions. Thereafter, oligo dT primed cDNAs were synthesized using the First Strand cDNA Synthesis Kit (GE Healthcare, Buckinghamshire, UK) following the manufacturer's instructions.

Quantitative RT–PCR

Quantitative RT–PCR (qRT–PCR) was performed on a Light-Cycler (Roche, Mannheim, Germany) using the QuantiTectTM SYBR® Green PCR kit (Qiagen, Hilden, Germany). Primers for the CXCL1, CXCL2, p65 (NFκB), IκBα, CXCR2, COX2, SPARC, ALDH3A1 and EFEMP1 target genes and for the housekeeping gene HPRT were designed using the Primer3 program and purchased from TibMolbiol (Berlin, Germany). All sequences are listed in Supplementary Table 1, available at *Carcinogenesis* Online. PCR conditions were set according to the manufacturer's instructions provided with the QuantiTectTM SYBR® Green PCR kit. All experiments were carried out in duplicates as recommended for the use of the LightCycler. The specificity of the RT–PCR products was proven by the appropriate melting curves (specific melting temperature) and by the expected size of the PCR products (data not shown). Expression data were normalized on the house keeping gene as indicated in the results section.

Western blots

Conditioned media from curcumin-treated (24 h) and respective non-treated control cells as well as conditioned media from p65-, IκBα-, CXCL1- or CXCL2-silenced and non-silenced control cells were analyzed using antibodies against CXCL1 and -2 (both from Dianova, Hamburg, Germany). Cellular extracts from p65-, IκBα-, CXCL1- or CXCL2-silenced and non-silenced control cells were analyzed using a p65, p-p65, IκBα, p-IκBα, COX2, SPARC and EFEMP antibodies (Cell Signalling, MA). For stimulation of IκBα phosphorylation cells were incubated with 10 µM TNFα (Sigma, Deisenhofen, Germany) prior to cell lysis. Likewise, for inhibition of IκBα phosphorylation 10 µM of a kinase β inhibitor (SC-514, EMD, Calbiochem, Gibbstown) was used in cell culture. Equal amounts of protein were subjected to sodium dodecyl sulfate–polyacrylamide gel electrophoresis and the intracellular amount of β-actin was analyzed as loading control (antibody from Sigma, Deisenhofen, Germany). For conditioned media, the amount of protein blotted onto the membranes was visualized with Ponceau red before blocking. Following electrophoretic separation by sodium dodecyl sulfate–polyacrylamide gel electrophoresis, proteins were electroblotted on nitrocellulose membranes (Whatman, Brentford, UK). The membranes were blocked in 5% non-fat milk (Merck, Darmstadt, Germany) overnight at 4°C. The first antibody was incubated for 1 h at room temperature. Thereafter, membranes were washed in Tris-buffered saline with Tween buffer, and a further incubation was carried out with a peroxidase-conjugated antibody (Dianova, Hamburg, Germany) for 1 h at room temperature. The enhanced chemiluminescence system was used for visualization of the protein bands as recommended by the manufacturer (Invitrogen, Carlsbad, CA). Blots were performed as described previously by us in detail (24). Semiquantitative evaluation of the bands was performed by densitometric analysis with the ImageJ software provided by the National Institutes of Health (http://rsb.info.nih.gov/ij/).

Apoptosis assay

Apoptotic cell death was determined by an enzyme-linked immunoassay (Cell Death Detection ELISA[PLUS]; Roche Applied Science, Mannheim, Germany) to detect fragmented DNA and histones (mononucleosomes and oligonucleosomes). Human prostate cancer cells PC-3 were seeded on 24-well plates and either transfected with siRNAs directed against CXCL1 and -2 and corresponding control oligos or treated with curcumin and corresponding carrier. All experiments were performed in triplicates. After an appropriate incubation period depending on the experiment, cells were washed with PBS, supernatants were collected for analysis of necrosis and cells were lysed and processed following the instructions of the manufacturer.

Immunofluorescence staining for NFκB p65 location

Cells were plated on SuperFrost glass slides for adherence and treated the next day with curcumin or transfected with siRNAs directed against CXCL1 and -2 and corresponding control oligos in triplicates. Slides were airdried for 1 h at room temperature and fixed with ice-cold acetone/methanol (1:1). After brief washing in PBS, slides were blocked with a blocking solution (Biogenex, San Ramon, CA) for 1 h and then incubated with a 1:100 dilution of rabbit polyclonal antihuman p65 antibody (Santa Cruz Biotechnology, Santa Cruz, CA). After overnight incubation, the slides were washed and then incubated with goat antirabbit IgG-Alexa 594 (Invitrogen—Molecular Probes, Carlsbad, CA) for 1 h and counterstained for nuclei with 1 µg/ml 4′,6-diamidino-2-phenylindole (DAPI) for 5 min. Stained slides were mounted with mounting medium (Vector Labs, Burlingame, CA) and analyzed under a fluorescence microscope with digital image capture (Leica, Bensheim, Germany).

Cell doubling

PC-3 cells were trypsinized and equal cell numbers were plated in 25 ccm flasks. The next day, cells were either treated with curcumin or transfected with small non-coding RNA oligos (siRNAs) specifically directed against CXCL1 and -2 or corresponding control oligos. After another incubation period of 1–5 days, cells were washed with PBS, trypsinized and the cell number was determined using a cell counter (Casy1TTC cell counter, Roche, Germany). All experiments were performed in triplicates.

Hematogenous metastases in immunodeficient mice

Animal studies and research protocols were reviewed and approved by the institutional ethics committee and were conducted in accordance with the national current regulations and guidelines for the care and use of laboratory animals (D.L. 27/01/1992, no. 116). Five-week-old CD-1 Foxn1[nu] male mice were obtained from Charles River Laboratories and were maintained under specific pathogen-free conditions and given sterile food and water *ad libitum*. Before intracardiac tumor inoculation, mice were anaesthetized with an intraperitoneal mixture of ketamine (50 mg/kg) and xylazine (5 mg/kg). Animal health and survival rate were observed until their euthanasia due to one of the following medical reasons: severe weights loss (exceeding 20% of original body mass), hyperventilation, paralysis or bone fracture. PC-3 cells were collected by trypsinization and washed and resuspended in PBS. Subsequently, 5×10^5 cells were injected into the heart of the mice. Mice were fed with LASCRdiet™ CRD55131 (LASvendi, Soest, Germany) containing 1% casein (controls) or 1% curcumin (Fluka, Buchs, Switzerland).

On day 35 after inoculation, mice were humanely killed. Following killing of the animals, all internal organs, including the brain, the vertebral column, humeri and femora were removed and immersed for 24–36 h in
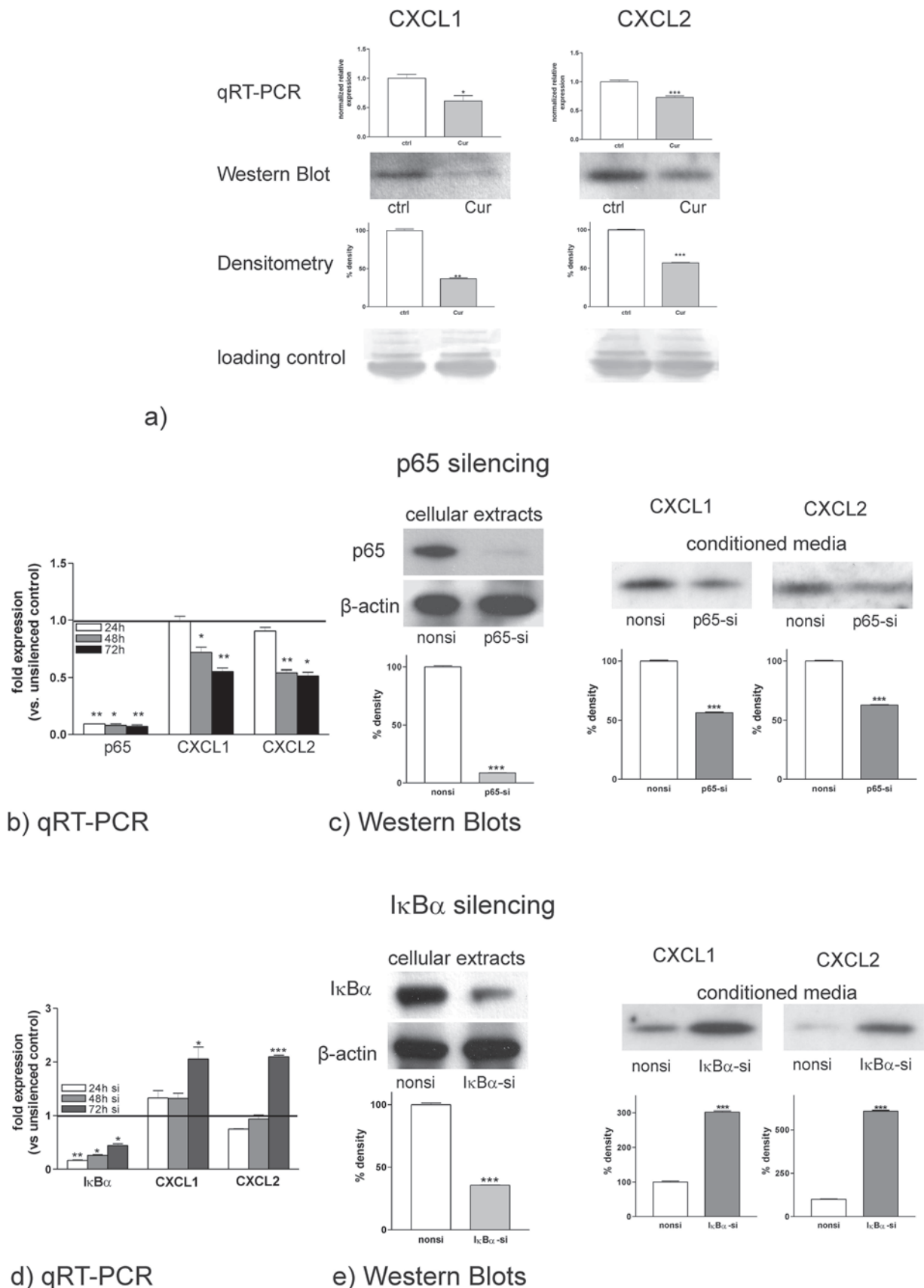
Fig. 1. Curcumin impairs the expression of CXCL1 and -2 via the NFκB signaling pathway. (**a**) Curcumin treatment of PC-3 cells (15 µM for 24 h) downregulates mRNA expression of CXCL1 by ~40% and that of CXCL2 by ~25% (upper panel indicated as 'qRT–PCR'). Statistical evaluation of the qRT–PCR results by Student's *t*-test resulted in *P* values of *P = 0.0101 for CXCL1 and ***P = 0.0002 for CXCL2. Western blot analysis reveals that CXCL1 protein secretion is diminished by >50% and that of CXCL2 by ~45% (panel indicated as 'western blot') compared with carrier-treated cells as evidenced by

buffered formaldehyde, pH 7.4. Subsequently, all material was dissected and completely embedded into paraffin as routinely performed. Samples containing bone were first decalcified in 0.1 M ethylenediaminetetraacetic acid until complete decalcification. Sections from all resulting tissue blocks were stained for hematoxylin and eosin. In addition, particular attention was paid to the dissection of the lungs resulting in all samples in a cross section through the largest diameter of the organs. Thereby, the pulmonary work up was standardized so that comparably sized cross sections through all lung samples were achieved. Following embedding into paraffin, serial sections were prepared from the lungs and were stained by immunohistochemistry in addition to the hematoxylin and eosin stain. The immunostainings comprised the localization of (human) cytokeratin (pan-keratin), p53 protein and the proliferation marker Ki-67 (all antibodies DAKO, Hamburg, Germany). All organ sections were analyzed by light microscopy and the presence and number of tumor cells/tumor cell aggregates were recorded. In the lung samples, all tumor cells/tumor cell aggregates present within the pulmonary parenchyma (intrapulmonary) were distinguished from those present at the pleural surface and/or seen in mediastinal soft tissue (peripulmonary). Metastases were identified by typical morphology, positive reaction for (human type) cytokeratin and enhanced proliferative capacity (Ki-67) or enhanced positivity of tumor cell nuclei for p53 protein. All metastases were counted irrespective of the metastasis size or the number of tumor cells present. The resulting metastasis frequencies were statistically evaluated.

Data analysis

Statistical significance was assessed by comparing mean (±SD) values, which were normalized to the control group with Student's *t*-test for independent groups. One-way analysis of variance (ANOVA) was used to test for statistical significance ($P < 0.05$), and when significance was determined, Bonferroni's multiple comparison test was performed *post hoc*, as indicated in the figure legends. Statistical analysis was performed using the Prism software (GraphPad, San Diego, CA).

Promoter analysis

The sequences 5000 bp upstream and 1000 bp downstream of the transcription start site of the genes CXCL1 (NM_001511.2), CXCL2 (NM_002089.3) and CXCR2 (NM_001557.3) were extracted using the human, mouse and rat promoter extraction service, PromoSer (http://biowulf.bu.edu/zlab/PromoSer/) (30); and analyzed using the transcription factor binding search tool TFSEARCH 1.3 (http://www.cbrc.jp/research/db/TFSEARCH.html) that identifies sequence elements that match to known transcription factor bindings sites stored in the Transfac database (31) and calculates a score ranging from 0 to 100 for sequences that divert from the consensus based on the degree of conservation of each single nucleotide. Matches with a score >85 were collected.

Results

Curcumin downregulates the inflammatory cytokines CXCL1 and -2 in metastatic prostate cancer by targeting NFκB signaling

We previously reported that curcumin inhibits the expression of the proinflammatory cytokines CXCL1 and -2 leading to diminished formation of breast cancer metastases (24). In this study, we show in a model of metastatic prostate cancer that curcumin downregulates the two cytokines by targeting the NFκB pathway and acting as kinase inhibitor.

The analysis of 281 human prostate cancers by microarray gene expression profiling (32) reveals that CXCL1 and -2 as well as CXCR2 are expressed in many human prostate cancers. The highly variable levels of expression (CXCL1—mean: 982.6, range 270.6–8192.0; CXCL2—mean: 2166.0, range 340.1–9607.9; CXCR2—mean 913.3, range 464–15825.9) probably reflecting differential inflammation status of these tissues (see Supplementary Figure 1, available at *Carcinogenesis* Online). We, therefore, analyzed expression of these cytokines and their receptors in human prostate cancer cell lines and found that among the commonly used prostate cancer cell lines, such as LNCaP, DU154 and PC-3, only PC-3 expressed CXCL1 and -2 as well as CXCR2 (see Supplementary Figure 1, available at *Carcinogenesis* Online). Therefore, we selected PC-3 cells as *in vitro* model for metastatic prostate cancer in our study.

In a first step, we investigated the effect of curcumin on the expression of CXCL1 and -2 mRNA (qRT–PCR) in metastatic prostate cancer cells PC-3. Treatment with the polyphenol ('Cur') for 24 h reduces statistically significantly CXCL1 transcription ~40% (Figure 1a, left upper panel) and CXCL2 transcription ~25% (Figure 1a, right upper panel) in comparison with the expression rate of PC-3 cells treated with the carrier alone (Figure 1a indicated with ctrl). Well in accordance with the transcription data, the corresponding protein levels (western blot) of CXCL1 and -2 were diminished in conditioned media of curcumin-treated PC-3 cells (Figure 1a, upper middle panel). The decrease of CXCL1 concentration 24 h after curcumin treatment in cell culture supernatants of curcumin-treated PC-3 cells was ~60% (Figure 1a, left side) and that of CXCL2 was ~50%. Densitometric analysis of the western blot data followed by statistical evaluation by Student's *t*-test revealed that the differences in CXCL1 and -2 amounts secreted into the cell culture supernatants between curcumin-treated and carrier-treated PC-3 cells were statistically highly significant. To assure that equal amounts of protein were subjected to the gels, we monitored the intensities of the bands on the nitrocellulose membranes by Ponceau red staining (Figure 1a, 'loading control').

In order to unravel the molecular mechanism behind the inhibitory effect of curcumin on CXCL1 and -2, we analyzed in depth the role of NFκB signaling in this context. Our previous studies using a model of metastatic breast cancer already exposed that p65 and IκBα are involved (24). Here, we extend our studies on metastatic prostate cancer and, moreover, we investigate the underlying regulation mechanism more in detail by going further upstream in the NFκB signaling pathway.

We analyzed the promoter regions of CXCL1, -2 and CXCR2 from 5000 bp upstream to 1000 bp downstream of the transcription start site. The promoters of CXCL1 and -2 share an almost identical proximal promoter region (92% identity in the region −137 to transcription start site) and no significant homology in distal promoter elements. This

←

densitometric evaluation of the band intensities (CXCL1: **$P = 0.0011$; CXCL2: ***$P = 0.0003$; Student's *t*-test). (**b**) The NFκB subunit p65 was transiently knocked down for 24, 48 and 72 h in PC-3 cells and quantitative RT–PCR analysis was performed to monitor the effects on CXCL1 and -2 expressions. All data are shown as fraction of values in cells transfected with siRNAs (*$P < 0.05$, **$P < 0.01$ and ***$P < 0.001$; analysis of variance with Bonferroni's multiple comparison test). Seventy-two hours after transfection the efficiency of p65 knockdown was ~90%, which resulted in decreased CXCL1 and -2 mRNA expressions rates down to ~50%. (**c**) Western blot analyses of cellular extracts from p65-silenced PC-3 cells (left panel) showed an ~10-fold reduction of p65 protein 72 h after transfection with siRNA targeted against p65 (lanes indicated with p65-si) in comparison with controls (lanes indicated with nonsi), which was statistically highly significant ($P < 0.0001$ targeted). To assure that equal amounts of total protein were loaded onto the gels, β-actin was used as a loading control (left lower panel). Western blot analyses of conditioned media of PC-3 cells harboring the knockdown of p65 (middle and right panel) revealed a 45% reduction of secreted CXCL1 and a 40% reduction of CXCL2 72 h after silencing (lanes indicated with p65-si) compared with controls (lanes indicated with nonsi). (**d**) The inhibitor of p65, IκBα was silenced for 24, 48 and 72 h in PC-3 cells to investigate whether CXCL1 and -2 expression was induced. CXCL1 and -2 mRNA expression data are shown as fraction of values in cells transfected with siRNAs (*$P < 0.05$, **$P < 0.01$ and ***$P < 0.001$; analysis of variance with Bonferroni's multiple comparison test). The knockdown of IκBα had an efficiency of ~70% after 24 h and faded out to ~50% after 72 h. mRNA levels for CXCL1 and -2 increased after IκBα knockdown with a maximum of ~2-fold expression after 72 h as compared with controls. (**e**) Western blot analyses of cellular extracts from IκBα-silenced PC-3 cells showed a 60% reduction of IκBα protein 72 h after transfection with specific siRNAs (lanes indicated with IκBα-si) in comparison with controls (lanes indicated with nonsi). The knockdown of IκBα had a statistical significance of $P = 0.0004$. To ensure equal amounts of total protein were subjected to the gels, β-actin was used as a loading control. Western blot analyses of conditioned media of PC-3 cells harboring the knockdown of IκBα (lanes indicated with IκBα-si) revealed a 3-fold increase of secreted CXCL1 and a 6-fold increase of CXCL2 after 72 h compared with controls (lanes indicated with nonsi). All experiments were performed at least in triplicates. Western blot results were quantified by densitometry followed by statistical analysis using Student's *t*-test. Statistical significances were *$P < 0.05$, **$P < 0.01$ and ***$P < 0.001$.
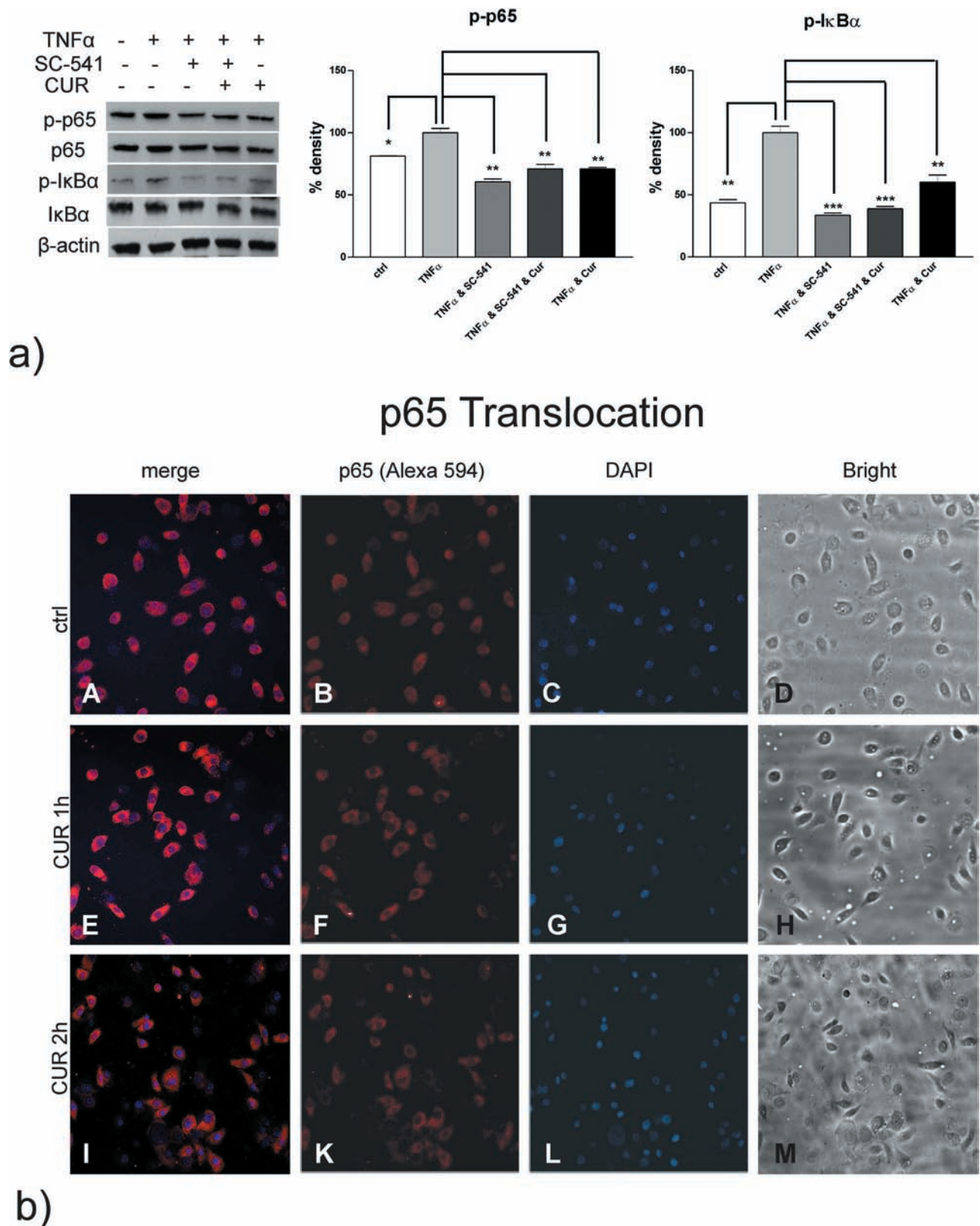
p65 Translocation

Fig. 2. Curcumin acts as kinase inhibitor in metastatic prostate cancer cells. (**a**, left panel) Phosphorylation of p65 and IκBα was stimulated in PC-3 cells for 10 min with TNFα, resulting in statistically significant 1.3-fold and 2.5-fold inductions of p-p65 and p-IκBα respectively. Phosphorylation of p65 could be diminished 1.7-fold after 2 h treatment with the commercial IκB kinase β inhibitor, SC-514. A similar effect could be achieved by treating PC-3 cells for 2 h with curcumin. Combined application of curcumin and SC-514 also led to inhibition of phosphorylation of p65, but the two drugs did not yield an additive or synergistic effect making a common inhibitory mechanism most likely. SC-514 diminished phosphorylation of IκBα 3-fold after 2 h. Curcumin led to a similar yet weaker reduction of IκBα phosphorylation. These results indicate that the polyphenol directly acts as an inhibitor of IκB kinase β. (**b**) Localization of the NFκB subunit p65 in different cellular compartments of PC3 cells was monitored by immunofluorescence using specific antibodies. In cells treated with the carrier alone, p65 was evenly distributed between cytoplasm and nucleus (A–C). One hour after curcumin treatment, p65 translocation into the nuclei was

region contains a perfect NFκB-binding site (GGGAATTTCC, −73 for CXCL1 and −75 for CXCL2). An additional, imperfect binding site is located close to the transcription start site in position −22 and −23. Further, imperfect binding sites are located in the 5′ upstream untranslated region for both genes. The CXCR2 promoter contains bona fide NFκB-binding sites 1071 and 1034 bp upstream and 85 bp downstream of the transcription start site (see Supplementary Table 2, available at *Carcinogenesis* Online).

In this context, we modulated the NFκB pathway in PC-3 cells by specifically silencing the gene transcription of p65 and IκBα by RNA interference. As determined by qRT–PCR 24, 48 and 72 h after transfection of the cells with small non-coding RNA oligos, we achieved knockdown efficiencies of up to 95% (after 72 h) for p65 and of up to 82% (after 24 h) for IκBα as compared with control cells transfected with non-target directed siRNAs (Figure 1b and 1d, columns indicated with p65 or IκBα respectively).

To verify the efficiency of gene silencing on protein level, we performed western blotting analysis of lysates. Consistent with our mRNA data, cellular extracts of p65- or IκBα-silenced PC-3 cells revealed an almost complete knockdown (~92%) of p65 protein (Figure 1c, left panel) and ~60% knockdown of IκBα protein (Figure 1e, left panel) 72 h after transfection with specific siRNAs as compared with cells transfected with a non-target directed siRNA.

As a consequence of p65 silencing, expression of CXCL1 and -2 mRNAs was statistically significantly diminished to a minimum of 60 and 55%, respectively, after 72 h (Figure 1b, columns indicated with 'CXCL1' and 'CXCL2').

As expected, silencing of IκBα in PC-3 cells led to a result opposed to that observed for p65 silencing and accordingly CXCL1 and -2 mRNA levels increased ~2-fold each 72 h after transfection as compared with control cells transfected with non-target-directed siRNAs (Figure 1d, columns indicated with 'CXCL1' and 'CXCL2').

Well in line with the results from qRT–PCR, protein levels of CXCL1 and -2 secreted into the conditioned media of PC-3 cells decreased when p65 was silenced (Figure 1c, middle and right panels) and augmented when IκBα was transiently knocked down (Figure 1e, right panels). The efficiency of transient gene silencing of p65 and IκBα by specific siRNAs was ~90% for both after 24 h on mRNA level (Figure 1b and 1d) and ~90 and 60%, respectively, after 72 h on protein level (Figure 1c and 1e, left panels). Amounts of secreted CXCL1 and -2 proteins diminished 45 and 40%, respectively, when p65 was silenced for 72 h as compared with control cells transfected with a nonsense oligo (Figure 1c, middle and right panels). On the contrary, CXCL1 and -2 levels increased 3-fold and 6-fold, respectively, when IκBα was transiently knocked down for 72 h (Figure 1e, middle and right panels). All differences found were statistically highly significant ranging from $P < 0.01$ up to $P < 0.001$ as indicated in the appropriate figures.

We furthermore wished to know whether curcumin inhibits phosphorylation and thereby functions as a kinase inhibitor in metastatic prostate cancer cells (Figure 2a). IκBα is phosphorylated by the inhibitor of the IκB kinase complex, mainly IKKβ. The effect of curcumin could, therefore, be due to inhibition of these kinases. We, therefore, compared the effects of curcumin with those obtained using the IκB kinase βinhibitor SC-514.

We stimulated phosphorylation of p65 and IκBα in PC-3 cells for 10 min with TNFα, resulting in statistically significant 1.3-fold and 2.5-fold inductions of p-p65 and p-IκBα respectively. Phosphorylation of p65 could be diminished 1.7-fold after 2 h treatment with SC-514. A similar effect could be achieved by treating PC-3 cells 2 h with curcumin. Combined application of curcumin and SC-514 also led to inhibition of phosphorylation of p65, but

the two drugs did not yield an additive or synergistic effect making a common inhibitory mechanism most likely. SC-514 diminished phosphorylation of IκBα 3-fold after 2 h. Curcumin led to a similar yet weaker reduction of IκBα phosphorylation. These results indicate that the polyphenol directly acts as an inhibitor of IκB kinase β.

In order to investigate whether the inhibitory effect of curcumin on phosphorylation of IκBα and p65 has a functional consequence on p65 translocation, we monitored the localization of this NFκB subunit in different cellular compartments by immunofluorescence using specific antibodies (Figure 2b). In PC-3 cells treated with the carrier alone, p65 was evenly distributed between cytoplasm and nucleus of the cells (A–C). Already 1 h after curcumin treatment, p65 translocation into the nuclei was impaired and the NFκB subunit remained in the cytoplasm of the prostate cancer cells (E–G). After 2 h treatment with curcumin, this effect became even more evident and most of the nuclei were free of p65 (I–L). DNA in the nuclei was stained with DAPI (C, G and L). Photographs of the cells using bright light show the morphology of the cells (D, H and M).

Taken together, these results show that curcumin acts as kinase inhibitor within the NFκB signaling cascade in metastatic prostate cancer cells. By blocking the phosphorylation of IκBα, curcumin has an effect further downstream on phosphorylation of p65, which in consequence impairs its translocation into the nucleus of the tumor cells (Figure 2). As a result, inhibition of NFκB leads to diminished expression rates of the proinflammatory cytokines CXCL1 and -2 (shown in Figure 1).

The proinflammatory cytokines CXCL1/-2 act in a feedback loop reversely on the NFκB pathway

Besides the regulatory effect of NFκB on CXCL1 and -2 expressions, we demonstrate here that the two inflammatory cytokines themselves act on single factors of the NFκB pathway (Figure 3). In detail, we first analyzed the silencing efficiency after transfection of the prostate cancer cells with siRNA oligos targeted specifically against CXCL1 and -2 (Figure 3a).

Compared with a non-silencing control (normalized expression level was set to 1 in qRT–PCR experiments, Figure 3a, upper panel) CXCL1 expression was downregulated ~60% after 24 and 48 h and ~50% after 72 h, whereas CXCL2 expression was inhibited ~85% after 24 h, 70% after 48 h and 60% after 72 h. On the corresponding protein level, CXCL1 and -2 expressions were silenced ~50 and 40%, respectively, as evidenced by western blots followed by densitometric analysis (Figure 3a, lower panels). All results were statistically highly significant with P values from $**P < 0.01$ to $***P < 0.001$ (Student's t-test).

We then show that silencing of CXCL1 and -2 downregulates p65 expression (Figure 3b, left upper panel), phosphorylation (Figure 3b, left lower panel) and translocation (Figure 3c), whereas it induces as expected the expression (Figure 3b, right upper panel) and block phosphorylation (Figure 3b, right lower panel) of the inhibitor of kappaB (IκBα).

Already 24 h after CXCL1 and -2 silencing, p65 mRNA expression was impaired ~25% with further highly statistically significant decrease ($P < 0.001$) down to ~80–90% after 72 h of silencing of the proinflammatory cytokines (Figure 3b, left upper panel). On the contrary, the expression of the inhibitor of p65 (IκBα) was 50% induced upon specific CXCL1 and -2 knockdown for 24 h. Prolonged silencing of CXCL1 for 48 h resulted in almost 2-fold increase of IκBα expression, whereas silencing of CXCL2 was most efficient after 72 h and led to a 2.5-fold increase of the same with a statistical significance of $P < 0.001$ (Figure 3b, right upper panel).

← impaired and p65 remained unphosphorylated in the cytoplasm (E–G). After 2 h treatment with curcumin this effect became even more evident and almost all nuclei were free of p65 (I–L). DNA in the nuclei was stained with DAPI (C, G and L). Photographs using bright light show the morphology of the cells (D, H and M). Magnification: ×20.
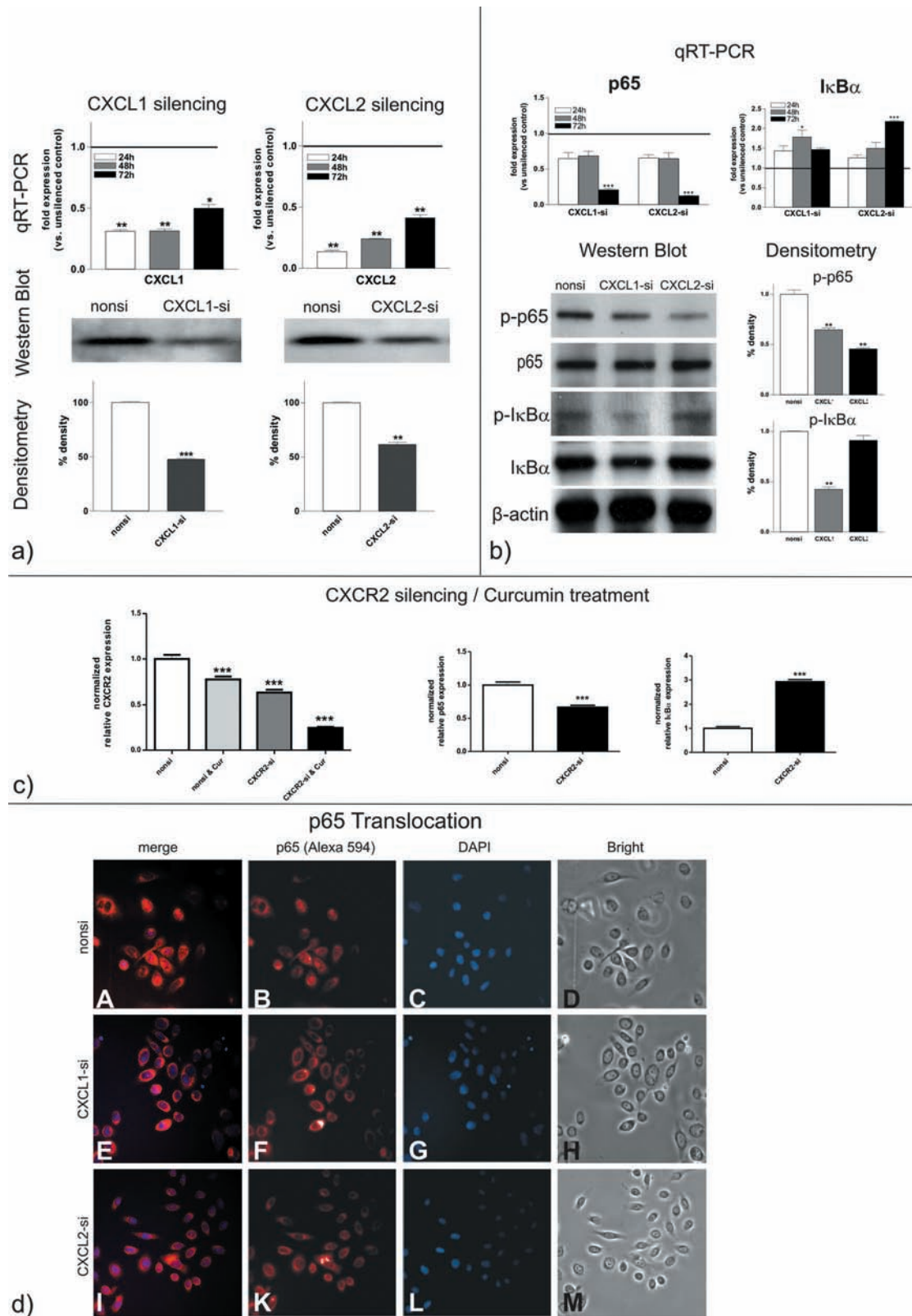
Fig. 3. CXCL1/-2 act in a feedback loop reversely on the NFκB pathway. (**a**) Silencing efficiency after transfection of the prostate cancer cells with siRNA oligos targeted specifically against CXCL1 and -2 compared with a non-silencing control was ~60% after 24 and 48h for CXCL1 and ~85% after 24h, 70% after 48h and 60% after 72h for CXCL2 mRNA expression (upper panels 'qRT–PCR'). On the protein level, CXCL1 and -2 expressions were silenced by ~50 and 40%, respectively, as evidenced by western blots followed by densitometric analysis (a, lower panels). All results were statistically highly significant with *P* values from **P < 0.01 to ***P < 0.001 (Student's *t*-test). (**b**) Twenty-four hours after CXCL1 and -2 silencing, p65 mRNA expression was impaired down to a minimum of 80–90% after 72h of silencing of the proinflammatory cytokines (left upper panel). In contrary, the expression of the inhibitor of p65 (IκBα) was induced upon specific CXCL1 and -2 knockdown up to a maximum of 2- and 2.5-fold after 48 and 72h, respectively (right upper panel). Densitometric analysis of the western blot data revealed that phosphorylation of p65 was diminished by ~40% by silencing of CXCL1 and by 55% by knocking down CXCL2. Phosphorylation of IκBα was only diminished by ~60% by gene knockdown of CXCL1, whereas the effect of silencing of CXCL2 was not significant. Results

2513

Densitometric analysis of the western blot data revealed that phosphorylation of p65 was diminished ~40% by silencing of CXCL1 and 55% by knocking down CXCL2. Phosphorylation of IκBα was only diminished ~60% by gene knockdown of CXCL1, whereas the effect of silencing of CXCL2 was not significant.

In order to investigate the involvement of the receptor of CXCL1 and -2, in feeding back on NFκB, we silenced CXCR2 by transient siRNA knockdown, and analyzed the effect on p65 and IκBα after 48 h by qRT–PCR (Figure 3c). Silencing efficiency on CXCR2 was ~40% (left panel) 48 h after transfection with specific siRNA oligos. Interestingly, 24 h curcumin treatment of the prostate cancer cells led to diminished CXCR2 expression (***$P < 0.001$) and the combination of CXCR2 silencing together with curcumin treatment had a synergistic effect on CXCR2 downregulation, which was most efficient after 48 h with ~75% (***$P < 0.001$). Well in line with our hypothesis, p65 expression was diminished ~40% (middle panel) and IκBα expression was induced ~3-fold (right panel).

As a consequence of diminished phosphorylation, p65 should not translocate into the nucleus and, therefore, we monitored the localization of this NFκB subunit in different cellular compartments after CXCL1 and -2 silencing (Figure 3d). In PC-3 cells transfected with a non-silencing control oligo (nonsi), p65 was evenly distributed between cytoplasm and nucleus of the cells (A–C). After CXCL1 silencing (CXCL1-si, E–G) as well as after CXCL2 silencing (CXCL2-si, I–L), p65 translocation into the nuclei is impaired and the NFκB subunit remains dephosphorylated in the cytoplasm of the prostate cancer cells. DNA in the nuclei was stained with DAPI (C, G and L). Photographs of the cells using bright light show the morphology of the cells (D, H and M)

CXCL1 and -2 inhibit growth and induce apoptosis in metastatic prostate cancer

We wished to know whether the effects of CXCL1 and -2 expressions on the tumor-progression-associated NFκB pathway translates directly into functional changes of tumor cell biology and, therefore, analyzed possible consequences of CXCL1 and -2 silencing on proliferation and apoptosis.

Cell doubling rates were remarkably diminished after curcumin treatment as well as after CXCL1 and -2 silencing within an observation period of up to 5 days (Figure 4a). Growth rates of cells were mostly diminished by curcumin treatment (open circle) with a rate of ~50% as compared with controls (open diamond). Likewise, silencing of CXCL1 (solid triangle) and CXCL2 (solid diamond) inhibited growth of prostate cancer cells ~45 and 35%, respectively. Statistical significance was ***$P < 0.001$ (Bonferroni).

Next, we examined the effect of CXCL1 and -2 expressions on their ability to induce apoptosis because this function is critical for suppression of tumor formation and metastasis.

Using quantitative RT–PCR technique, we analyzed CXCL1- and -2-silenced human metastatic prostate cancer cells PC-3 for expression of the apoptosis-related factors bcl2 and survivin/birc5 and compared the effect of CXCL1 and -2 expression with that of curcumin treatment in an experiment performed in parallel (Figure 4b). Statistically significant downregulation (*$P < 0.05$, **$P < 0.01$, ***$P < 0.01$; ANOVA with Bonferroni's posttest) of the two survival-related factors bcl2 and survivin/birc5 could be achieved 72 h after transfection

with small non-coding RNAs directed against CXCL1 and -2, yet to a different extent. Although CXCL1 silencing led to a downregulation of 55 and 65% for bcl2 and birc5, respectively, CXCL2 inhibited bcl2 expression by ~60% and that of birc5 only by 10%. Curcumin treatment for 24 h inhibited bcl2 expression by ~50% and birc5 expression by ~60%, when compared with PC-3 cells treated with only the carrier.

Functional apoptosis/necrosis assays revealed that CXCL1 and -2 silencing leads to enhanced apoptosis ('Apo') and necrosis ('Nec') (Figure 4c) in a highly statistically significant manner (*$P < 0.05$, **$P < 0.01$ and ***$P < 0.001$; ANOVA with Bonferroni's posttest). By silencing of CXCL1 and -2 for 72 h in human metastatic prostate cancer cells PC-3, apoptosis rate could be almost doubled as compared with PC-3 cells transfected with an appropriate control oligo (Figure 4c, left side 'Apo'). Similarly, necrosis rate was significantly statistically increased in CXCL1- and -2-silenced PC-3 cells as compared with an appropriate control (Figure 4c, right side 'Nec'). Comparing the effect of CXCL1 and -2 silencing to curcumin treatment after 72 h, we found that the polyphenol acts more weakly on apoptosis with an induction rate of 50%, but more strongly on necrosis with an induction rate of 60%.

Curcumin downregulates metastatic factors via CXCL1 and -2

In order to investigate whether curcumin reduces the metastatic potential of prostate cancer cells, we analyzed the expression of a series of metastasis-related genes after treatment of metastatic PC-3 cells with the polyphenol (Figure 5a). We chose genes whose functional involvement has been shown through the analysis of highly metastatic tumor cells with pulmonary tropism (33). After 24 h of curcumin treatment, mRNA expression of the metastasis-related genes SPARC (osteonectin), COX2 (PTGS2, prostaglandin-endoperoxide-synthase 2), ALDH3A1 (aldehyde-dehydrogenase 3 family member A1) and EFEMP (EGF-containing fibulin-like extracellular matrix protein 1) was statistically significantly (**$P < 0.01$, ***$P < 0.001$, Student's *t*-test) diminished, whereby downregulation was most efficient for COX2 with a reduced expression level down to ~45% in curcumin-treated cells as compared with carrier-treated cells (Figure 5a, left graph 'qRT–PCR'). On the corresponding protein level, curcumin downregulated COX 2 ~50% (**$P < 0.01$), SPARC ~25% (***$P < 0.001$) and EFEMP1 ~40% as evidenced by western blots followed by densitometry (Figure 5a, middle and right panels).

We furthermore asked whether inhibition of the two proinflammatory cytokines can affect the metastatic potential of the cells. To answer this question, we analyzed the expression of metastasis-related genes in CXCL1- and -2-silenced PC-3 cells. We demonstrate that 72 h silencing of the two cytokines is followed by downregulation of SPARC, COX2, ALDH3A1 and EFEMP as evidenced by qRT–PCR (Figure 5b, left panel). Transcription of COX2 and SPARC, which were already among the most downregulated factors by curcumin, was reduced by ~75% and 50–80%, respectively, by transiently knocking down the expressions of the two cytokines. Interestingly ALDH3A1 mRNA synthesis, which was inhibited by curcumin only by 25%, was almost abolished by CXCL1 and -2 silencing.

Impaired expression of COX2, SPARC and EFEMP1 could also be seen on the level of the corresponding proteins. Our western blot results after 72 h of CXCL1 or CXCL2 silencing in PC-3 cells (Figure 5b, middle panel; lanes indicated with CXCL1-si and CXCL2-si,

---

← were statistically significant with *P* values of *$P < 0.05$, **$P < 0.01$ and ***$P < 0.001$ (Student's *t*-test). (**c**, left panel) CXCR2 expression is downregulated ~20% upon 24 h of curcumin treatment and ~30% upon 48 h of CXCR2 silencing; combination of CXCR2 silencing together with curcumin treatment for 48 h resulted in a 70% diminished CXCR2 expression. (c, middle panel) Expression of the NFκB subunit p65 was impaired upon 48 h of CXCR2 silencing in PC3 cells. (c, right panel) Well in line, IκBα expression was induced 3-fold upon 48 h CXCR2 silencing. All results were statistically highly significant (one-way ANOVA, with Bonferroni's multiple comparison test *post hoc* ***$P < 0.001$). All experiments were performed in triplicates. (**d**) Localization of p65 was monitored in different cellular compartments after 48 h of CXCL1 and -2 silencing. In PC-3 cells transfected with a non-silencing control oligo (nonsi), p65 was evenly distributed between cytoplasm and nucleus of the cells ('nonsi', A–C). After CXCL1 ('CXCL1-si', E–G) and CXCL2 silencing ('CXCL2-si', I–L), p65 translocation into the nuclei was impaired and the NFκB subunit remained in the cytoplasm of the prostate cancer cells. DNA in the nuclei was stained with DAPI (C, G and L). Photographs using bright light show the morphology of the cells (D, H and M). Magnification: ×20.

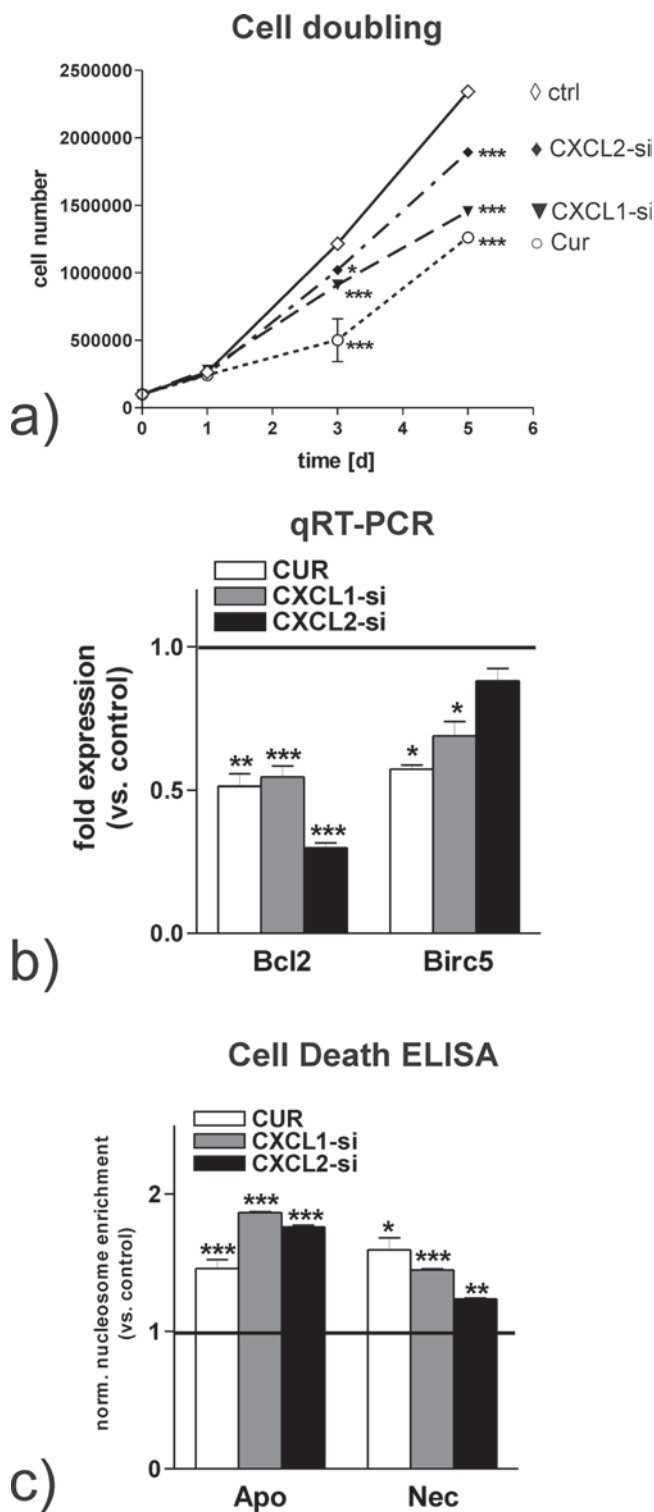## Cell doubling

a)

qRT-PCR

b)

Cell Death ELISA

c)

respectively) followed by densitometric analysis (Figure 5b, right panel) demonstrate that COX2 and SPARC expressions were statistically significantly abrogated by ~50 and 60%, respectively, in cell lysates 72 h after transfection with the specific oligo directed against CXCL1 when compared with cells transfected with a non-silencing oligo (lanes indicated with nonsi). The same effect could be observed in CXCL2-silenced PC-3 cells, but to a much weaker extend. In this study, COX2 and SPARC expressions were diminished only by ~10 and 30% when compared with cells transfected with a non-silencing oligo (lanes indicated with nonsi); however, with statistical significances of $**P < 0.01$ and $***P < 0.001$, respectively (Student's t-test). A weak downregulation of EFEMP1 protein of ~15% could only be achieved by CXCL2 silencing (Figure 5b, middle and right panel). Intracellular β-actin levels were monitored as a loading control.

Metastatic process in prostate cancer is driven by the CXCL1/-2—NFκB axis

In order to further investigate the involvement of NFκB in regulating the metastatic potential of prostate cancer cells through CXCL1 and -2, we complemented the list of genes altered after IκBα silencing (Figure 1d and 1e) with the metastasis-related genes COX2 and SPARC (Figure 5c). In accordance with the knockdown of IκBα, mRNA expression levels of both genes significantly increased ($**P < 0.01$, $**P < 0.001$). Although the expression of COX2 was induced >40-fold, 72 h after IκBα silencing, SPARC expression was upregulated a~2.5-fold when compared with control cells that were transfected with a non-target-directed siRNA (nonsi). Similar to CXCL1 and -2, the rise in the expression of the metastasis-related genes, COX2 and SPARC, can be attributed to the increased activation of NFκB, which is caused by the lack of its inhibitor IκBα, leading to an elevated metastatic potential of the prostate cancer cells.

Metastasis of prostate cancer xenografts is reduced by curcumin

Subconfluent PC-3 cells (5×10^5) were injected into the heart of nude mice that were subsequently divided into two groups that received standard or curcumin diets. This route of administration, although leading to suboptimal absorption of the polyphenol that is mainly excreted with the feces, was chosen in consideration of the probable route of administration for dietary chemopreventive agents. Mice were observed for 5 weeks within which period the two groups did not show any differences, especially, curcumin-treated mice did not reveal any side effects of the treatment, and the weights of the animals of the two groups were comparable. After 5 weeks, mice were killed and all internal organs, the vertebral column and both humeri and femora were collected and examined.

Lung metastases were counted after preparation of eosin–hematoxylin stained paraffin sections. In both study groups, tumor cells/cell aggregates were seen in the intrapulmonary and the peripulmonary compartments, though to different numbers. Peripulmonary metastases are more likely to be derived from direct dissemination during the intercardiac injection. We, therefore, limited our analysis to intrapulmonary metastases that are of hematogenous origin. The tumor cell morphology showed characteristic atypia.

Fig. 4. CXCL1 and -2 inhibit growth and induce apoptosis in metastatic prostate cancer. (**a**) After 5 days, growth rates of cells were most strongly reduced by curcumin treatment (open circle) with a rate of ~50% as compared with controls (open diamond). Likewise, silencing of CXCL1 (solid triangle) and -2 (solid diamond) inhibited growth of prostate cancer cells by ~45 and 35%, respectively. Statistical significance was $***P < 0.001$ (Student's t-test). (**b**) Statistically significant downregulation ($*P < 0.05$, $**P < 0.01$, $***P < 0.01$; ANOVA with Bonferroni's posttest) of the two survival-related factors, bcl2 and survivin/birc5, could be achieved 72 h after transfection with small non-coding RNAs directed against CXCL1 and -2. CXCL1 silencing led to a downregulation of 55 and 65% for bcl2 and birc5, respectively, whereas CXCL2 inhibited bcl2 expression by ~60%

and that of birc5 by only 10%. Treatment with curcumin for 24 h inhibited bcl2 expression ~50% and birc5 expression by ~60%, when compared with PC-3 cells treated with only the carrier. (**c**) CXCL1 and -2 silencing leads to enhanced apoptosis ('Apo') as well as necrosis ('Nec') in a highly statistically significant manner ($*P < 0.05$, $**P < 0.01$, $***P < 0.001$; ANOVA with Bonferroni's posttest). By silencing of CXCL1 and -2 for 72 h in human metastatic prostate cancer cells PC-3, apoptosis rate could be almost doubled as compared with PC-3 cells transfected with an appropriate control oligo (left side, 'Apo'). Similarly, necrosis rate was significantly increased in CXCL1 and -2 silenced PC-3 cells as compared with an appropriate control (right side, 'Nec'). Comparing the effect of CXCL1 and -2 silencing to curcumin treatment for 72 h, we found that the polyphenol acts more weakly on apoptosis with a induction rate of 50%, but more strongly on necrosis with a induction rate of 60%.
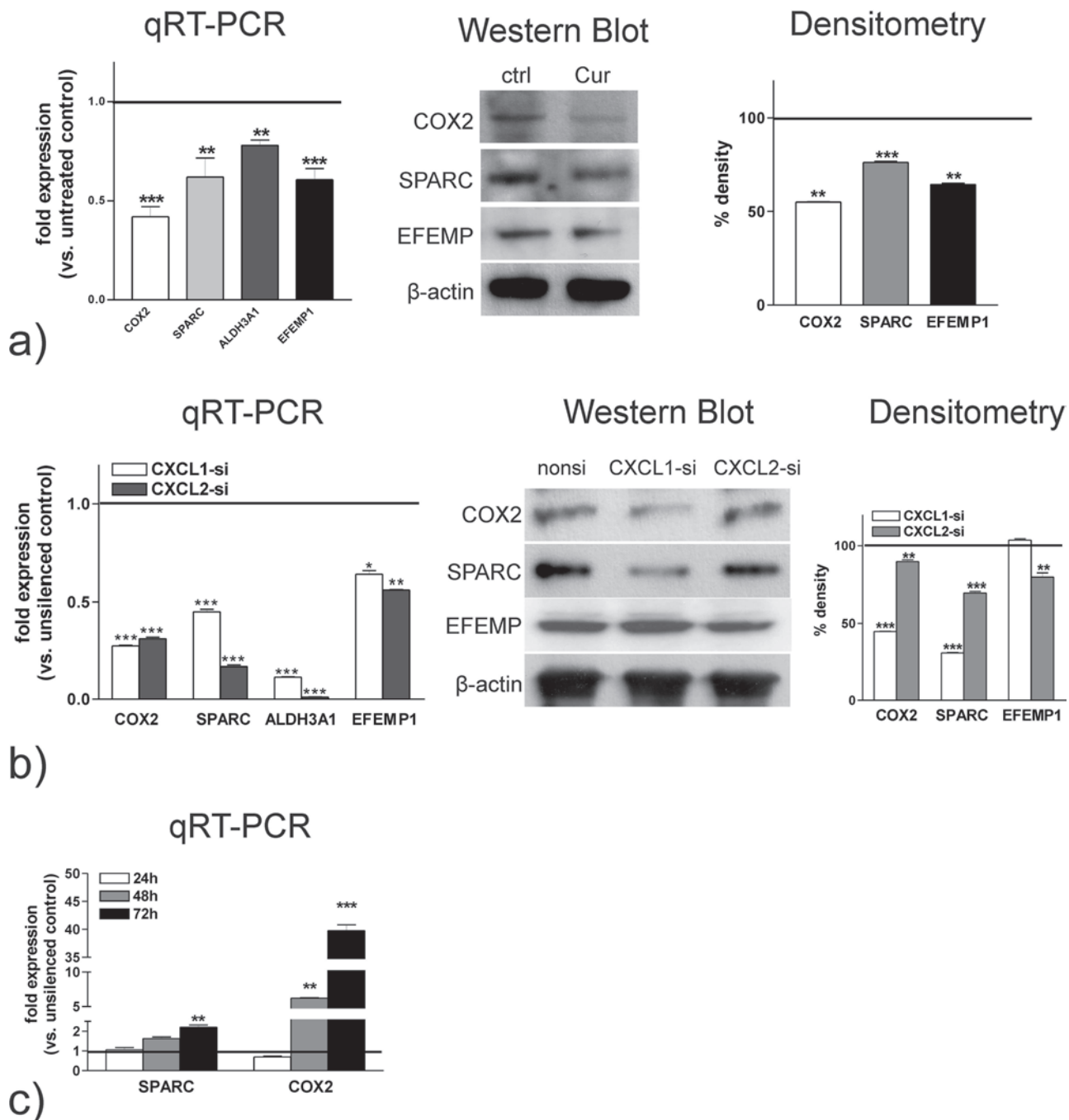
Fig. 5. Curcumin downregulates metastatic factors via CXCL1 and -2. (**a**, left panel, 'qRT–PCR') After 24 h curcumin treatment, mRNA expression of SPARC, COX2, ALDH3A1 and EFEMP was statistically significantly (**$P < 0.01$, ***$P < 0.001$; Student's t-test) downregulated in curcumin-treated cells as compared with carrier-treated cells. (a, middle and right panel) On the corresponding protein level, 24 h curcumin treatment downregulated COX 2 by ~50% (**$P < 0.01$), SPARC by ~25% (***$P < 0.001$) and EFEMP1 by ~40% (western blots followed by densitometry). (**b**, left panel, 'qRT–PCR') Silencing of the CXCL1 and -2 leads to downregulation of SPARC, COX2, ALDH3A1 and EFEMP. Inhibition of metastatis correlated factors in prostate cancer cells was more pronounced in CXCL2- than in CXCL1-silenced cells, at least for SPARC, ALDH3A1 and EFEMP. ALDH3A1 mRNA synthesis, which was reduced by curcumin only 25%, was almost abolished by CXCL1 and -2 silencing. (b, middle and right panel) Impaired expression of COX2, SPARC and EFEMP1 could also be seen on the level of the corresponding proteins. COX2 and SPARC expressions were statistically significantly abrogated by ~50 and 60%, respectively, in cell lysates 72 h after transfection with the specific oligo directed against CXCL1 (lanes indicated with CXCL1-si). Likewise COX2 and SPARC expressions were diminished only by ~10 and 30% after CXCL2 silencing (lanes indicated with CXCL2-si) as compared with cells transfected with a non-silencing oligo (lanes indicated with nonsi). A weak downregulation of EFEMP1 protein of ~15% could only be achieved by CXCL2 silencing. All results were statistically significant with *$P < 0.05$, **$P < 0.01$ and ***$P < 0.001$ (Student's t-test). Intracellular β-actin levels were monitored as a loading control. Metastatic process in prostate cancer is driven by the CXCL1/2–NFκB axis. (**c**) mRNA expression levels of the metastasis-related genes COX2 and SPARC increased statistically highly significantly (**$P < 0.01$, **$P < 0.001$) after knockdown of IκBα by RNAi technique. Although the expression of COX2 was induced >40-fold, 72 h after IκBα silencing, SPARC expression was upregulated ~2.5-fold when compared with control cells that were transfected with a non-target-directed siRNA (nonsi).
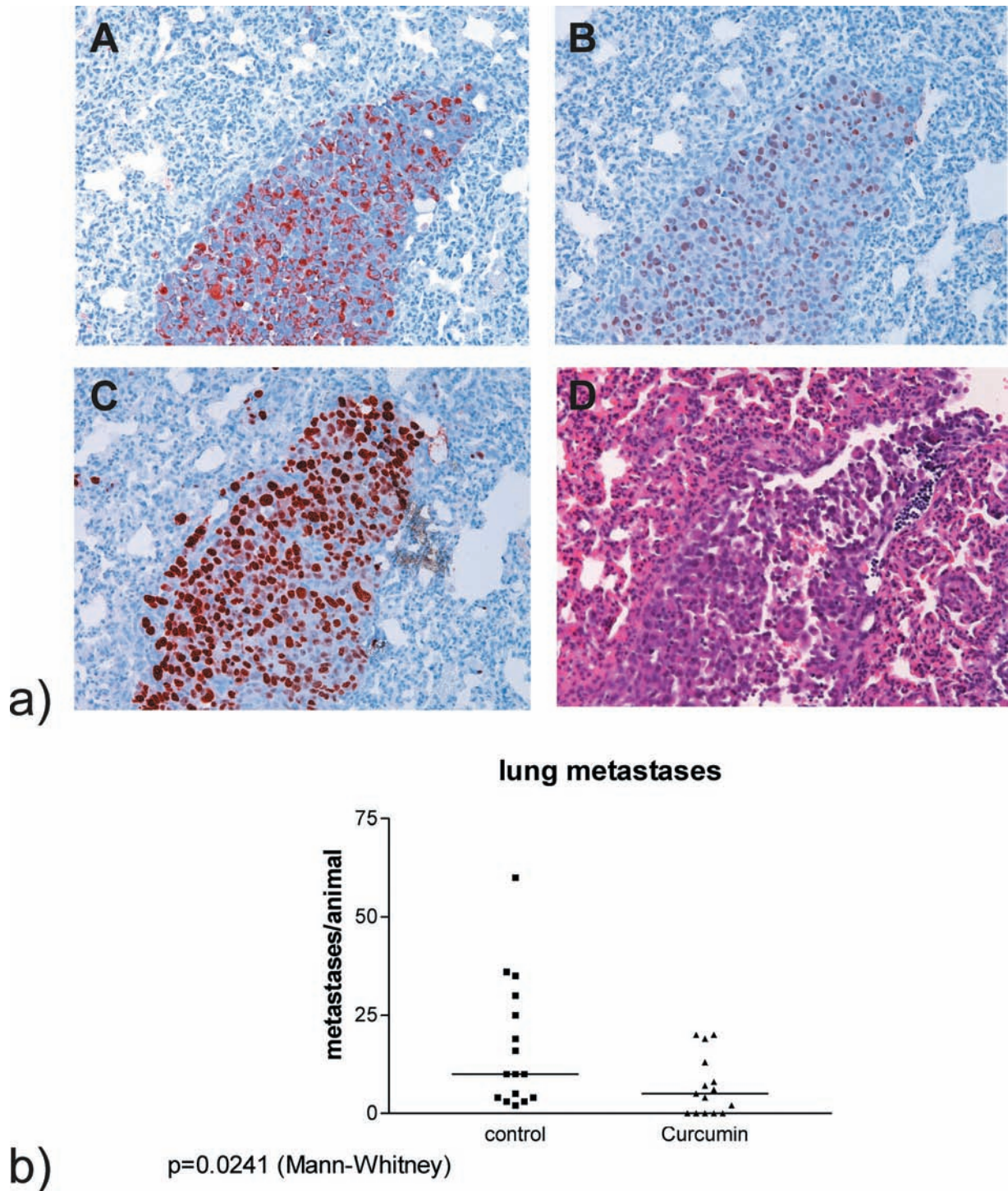
Fig. 6. Mouse metastasis of prostate cancer xenografts is reduced by curcumin. PC3 cells (5×10^5) were injected into the heart of immunodeficient mice. Animals were untreated (control) or treated with curcumin in the diet and killed after 5 weeks. Lungs were removed, fixed and four sections for each animal were analyzed for metastases. (**a**) Histology of metastases formed. The immunolocalization of (human) cytokeratin in the periphery of a mouse lung specimen reveals multiple selectively and positively stained tumor cells and small tumor cell aggregates (brown color) (A, antihuman cytokeratin). Immunohistochemical staining for p53 protein of a mouse lung specimen also shows multiple positively labeled cell nuclei (brown color) indicating implanted prostate cancer metastases (B, antihuman p53 protein). Localization of the cell proliferation antigen Ki-67 with positive labeling of isolated tumor cell groups (brown color) shows cell proliferation of the transplanted tumor cells [C, antihuman Ki-67 antigen (MIB-1)]. The overview of lung tissue 5 weeks after intracardiac tumor cell injection shows small groups of cells with typical morphological features of tumor cells (polymorphism, atypia, mitotic activity) (D, H, and E). Original magnification: × 400. (**b**) Number of metastases formed. The scattergrams report the numbers of metastases found in each of the untreated (control, $n = 16$) and curcumin treated (curcumin; $n = 15$) animals (mean of four sections analyzed). Mean number of metastases per animal are reduced in curcumin-treated animals. Note the high number of animals with no or very few metastases in treated animals (Mann–Whitney, $P = 0.0241$).

Significant expression of human p53 protein was observed only in tumor cells. Vitality of the tumor cells was confirmed by a high number (80–90%) of proliferating Ki-67 positive cells, thus excluding tumor cell dormancy (Figure 6a).

Tumors of treated and untreated animals were similar in dimension, morphology and histology. Figure 6b demonstrates that curcumin prevented the formation of lung metastases in a highly significant manner (Mann–Whitney test, $P = 0.0241$). The effect of curcumin on lung metastasis becomes also evident from Supplementary Table 3, available at *Carcinogenesis* Online that shows the mice subdivided in ranks with no, few (<10) and many (>10) metastases. The number of animals with few metastases (<10) was increased in treated (11 of 15 animals; 74%) as compared with untreated animals (9 of 16 animals; 55%). Five curcumin-treated and none of the control animals remained metastases free. Seven controls and only four treated animals had high total metastases counts (>10).

Discussion

Many studies have shown anticancer effects of curcumin (1,34). Given the widespread use of curcumin as a spice and in consideration of the absence of toxicity even of high dosages, the use of the polyphenol for chemoprevention has been proposed. Cancer patients who have obtained adjuvant therapy and faced a residual risk of relapse might wish to continue a non-toxic preventive therapy after adjuvant therapy. Finally, the introduction of more sophisticated prognostic procedures might induce low-risk cancer patients to opt against chemotherapy leaving room for non-toxic preventive treatments (35).

In this study, we address the specific situation of prostate cancer. Benign prostate hyperplasia and prostate *in situ* neoplasia are potential precursor lesions of prostate cancer although it is not clear whether there is a continuity between these situations (36,37). In addition, many elderly men have prostate cancer but do not know it and the recent recommendation against prostate cancer (prostate-specific antigen) screenings (38) in men >65 years old, which is going to be extended to younger men (39) suggests the introduction of dietary integrators that lower the risk of prostate cancer or its progression to clinically overt and eventually metastatic disease. These situations justify preventive treatments that target the potential of prostate (cancer) cells to grow and to metastasize.

Curcumin is a plant-derived compound that is particularly suited for prevention of prostate cancer formation and progression because it is known to act on the central activator of inflammation, NFκB, and prostate hyperplasia and cancer are known to be driven by inflammation (25). Yet, the inflammatory forms of prostate cancer are far from being as aggressive as, for example, inflammatory breast cancer that will hardly respond to bland chemopreventive drugs.

Several studies have shown effects of curcumin on prostate cancer cell survival through the downregulation of antiapoptotic survival genes *in vitro* (40,41) and *in vivo* (42,43) as well radiosensitizing effects (6,44). The effects on the highly aggressive androgen-independent prostate cancer cell line PC-3 have also been analyzed (6,43) (see also ref. (45)). We have chosen this model assuming that if curcumin can reduce formation of metastases by PC-3 cells, similar effects in less aggressive forms of cancer become even more likely.

We show that curcumin acts on the activation of NFκB through the stabilization of IκB in prostate cancer cells just like it has been shown for other cells (for a review, see ref. (46)). Inhibition of IκK appears to be the true mechanism because curcumin shows similar effects as the synthetic inhibitor SC-514, but administration of both SC-514 and curcumin does not lead to additive or synergistic effects.

Similar to what we have previously observed in breast cancer cells, curcumin downregulates the inflammatory cytokines CXCL1 and -2. We show that both cytokines are under the control of NFκB because transcriptional silencing of the NFκB subunit p65 leads to reduced expression, whereas silencing of IκB leads to increased expression of the cytokines. None of the two cytokines is listed as a known target of NFκB in man, CXCL2 is listed as a target in mouse [http://bioinfo.lifl.fr/NF-KB/; http://www.bu.edu/nf-kb/gene-resources/target-genes/;

see also ref. (47)]. We also show for the first time that the two cytokines establish a positive feedback loop inasmuch as phosphorylation of p65 and IκBα was reduced in cells where the expression of the cytokines was abolished by siRNA silencing. Diminished phosphorylation of IκBα stabilizes the inhibitor which in turn reduces phosphorylation of p65 and blocks the NFκB complex in the cytoplasm as evident from immunofluorescence analyses. The feedback appears to be mediated by CXCR2, the receptor for the two cytokines, because its silencing reduces p65 transcription and phosphorylation, similar to what we observed after treatment with curcumin. CXCR2 has been shown to mediate resistance to chemotherapy that induces an autocrine NFκB/cytokine feedback loop (48) that, as we show here, is interrupted by curcumin. Knockdown of CXCR2 has been described to reduce the invasive potential and the number of metastases formed by xenografts of breast cancer cells (49). CXCR2 itself is regulated by NFκB in prostate cells (50) and, as expected, responds to the treatment with curcumin as we show here. It is, therefore, most likely that the observed effect of curcumin on the formation of metastases is at least in part due to the interruption of the feedback loop that involves CXCR2.

Treatment of PC-3 cells with curcumin and silencing of CXCL1 and -2 reduce cell growth. The antiapoptotic molecules BCL2 and BIRC5/survivin are downregulated by curcumin and by CXCL1 and -2 silencing. This explains the induction of apoptosis that we observed in our experiments. Antiapoptotic effects of curcumin also determine its radio- and chemosensitizing effects (51).

In addition, curcumin downregulates COX2 (PTGS2) whose overexpression has also been linked to prostate hyperplasia (28,52). COX2 is a known NFκB-dependent mediator of inflammation and has already been identified as a target of other chemopreventive compounds (12,53).

Taken together, these data delineate the molecular mechanisms by which curcumin reduces survival and growth of prostate cancer cells on the one hand, and the ability of the cells to form metastases on the other hand. Curcumin interrupts an important positive feedback loop between the cytokines and NFκB that is responsible for the activation of several mediators of metastasis. This is particularly important in prostate cancer because inflammation plays a crucial role in its progression toward more aggressive growth and metastasis.

Indeed, our *in vivo* experiment demonstrates that curcumin-treated animals show a significant reduction in the number of lung metastases formed from circulating prostate cancer cells after intracardial injection into the left ventricle. In the group of curcumin-treated animals, but not in the control group, several animals remain metastasis free despite the large number of cells injected. The hematogenous metastasis assay specifically addresses the capacity of the cells to extravasate and to colonize a target tissue and the number of metastases formed is a direct measure of the metastatic potential.

Curcumin, therefore, appears particularly suited for prostate cancer prevention in healthy elder men, in patients with benign prostate hyperplasia and eventually low-grade prostate cancers in elder patients where 'watchful waiting' might remain an option.

Supplementary material

Supplementary Tables 1–3 and Figure 1 can be found at http://carcin.oxfordjournals.org/

References

1. Bachmeier,B.E. *et al.* (2010) Novel aspects for the application of Curcumin in chemoprevention of various cancers. *Front. Biosci. (Schol. Ed).*, **2**, 697–717.

2. Johnson,J.J. *et al.* (2007) Curcumin for chemoprevention of colon cancer. *Cancer Lett.*, **255**, 170–181.

3. Bachmeier,B. *et al.* (2007) The chemopreventive polyphenol Curcumin prevents hematogenous breast cancer metastases in immunodeficient mice. *Cell. Physiol. Biochem.*, **19**, 137–152.

4. Wilken,R. *et al.* (2011) Curcumin: A review of anti-cancer properties and therapeutic activity in head and neck squamous cell carcinoma. *Mol. Cancer*, **10**, 12.

5. Moghaddam,S.J. *et al.* (2009) Curcumin inhibits COPD-like airway inflammation and lung cancer progression in mice. *Carcinogenesis*, **30**, 1949–1956.

6. Chendil,D. *et al.* (2004) Curcumin confers radiosensitizing effect in prostate cancer cell line PC-3. *Oncogene*, **23**, 1599–1607.

7. Dance-Barnes,S.T. *et al.* (2009) Lung tumor promotion by curcumin. *Carcinogenesis*, **30**, 1016–1023.

8. Singh,S. *et al.* (1995) Activation of transcription factor NF-kappa B is suppressed by curcumin (diferuloylmethane) [corrected]. *J. Biol. Chem.*, **270**, 24995–25000.

9. Jobin,C. *et al.* (1999) Curcumin blocks cytokine-mediated NF-kappa B activation and proinflammatory gene expression by inhibiting inhibitory factor I-kappa B kinase activity. *J. Immunol.*, **163**, 3474–3483.

10. Bharti,A.C. *et al.* (2003) Curcumin (diferuloylmethane) down-regulates the constitutive activation of nuclear factor-kappa B and IkappaBalpha kinase in human multiple myeloma cells, leading to suppression of proliferation and induction of apoptosis. *Blood*, **101**, 1053–1062.

11. Balkwill,F. *et al.* (2001) Inflammation and cancer: back to Virchow? *Lancet*, **357**, 539–545.

12. Pfeffer,U., *et al.* (2005) Molecular mechanisms of action of angiopreventive anti-oxidants on endothelial cells: microarray gene expression analyses. *Mutat Res*, **591**, 198–211.

13. Wang,C.Y. *et al.* (1999) Control of inducible chemoresistance: enhanced anti-tumor therapy through increased apoptosis by inhibition of NF-kappaB. *Nat. Med.*, **5**, 412–417.

14. Sung,B. *et al.* (2009) Curcumin circumvents chemoresistance *in vitro* and potentiates the effect of thalidomide and bortezomib against human multiple myeloma in nude mice model. *Mol. Cancer Ther.*, **8**, 959–970.

15. Dhandapani,K.M. *et al.* (2007) Curcumin suppresses growth and chemoresistance of human glioblastoma cells via AP-1 and NFkappaB transcription factors. *J. Neurochem.*, **102**, 522–538.

16. Saini,S. *et al.* (2011) Curcumin modulates microRNA-203-mediated regulation of the Src-Akt axis in bladder cancer. *Cancer Prev. Res. (Phila).*, **4**, 1698–1709.

17. Collett,G.P. *et al.* (2004) Curcumin induces c-jun N-terminal kinase-dependent apoptosis in HCT116 human colon cancer cells. *Carcinogenesis*, **25**, 2183–2189.

18. Garg,R. *et al.* (2008) Curcumin decreases 12-O-tetradecanoylphorbol-13-acetate-induced protein kinase C translocation to modulate downstream targets in mouse skin. *Carcinogenesis*, **29**, 1249–1257.

19. Elamin,M.H. *et al.* (2010) Curcumin inhibits the Sonic Hedgehog signaling pathway and triggers apoptosis in medulloblastoma cells. *Mol. Carcinog.*, **49**, 302–314.

20. Bachmeier,B.E. *et al.* (2010) Reference profile correlation reveals estrogen-like transcriptional activity of Curcumin. *Cell. Physiol. Biochem.*, **26**, 471–482.

21. Sharma,R.A. *et al.* (2007) Pharmacokinetics and pharmacodynamics of curcumin. *Adv. Exp. Med. Biol.*, **595**, 453–470.

22. Hassaninasab,A. *et al.* (2011) Discovery of the curcumin metabolic pathway involving a unique enzyme in an intestinal microorganism. *Proc. Natl. Acad. Sci. U.S.A.*, **108**, 6615–6620.

23. Hoehle,S.I. *et al.* (2007) Glucuronidation of curcuminoids by human microsomal and recombinant UDP-glucuronosyltransferases. *Mol. Nutr. Food Res.*, **51**, 932–938.

24. Bachmeier,B.E. *et al.* (2008) Curcumin downregulates the inflammatory cytokines CXCL1 and -2 in breast cancer cells via NFkappaB. *Carcinogenesis*, **29**, 779–789.

25. De Marzo,A.M. *et al.* (2007) Inflammation in prostate carcinogenesis. *Nat. Rev. Cancer*, **7**, 256–269.

26. Abdollah,F. *et al.* (2011) Cancer-specific and other-cause mortality after radical prostatectomy versus observation in patients with prostate cancer: competing-risks analysis of a large North American population-based cohort. *Eur. Urol.*, **60**, 920–930.

27. Schenk,J.M. *et al.* (2010) Biomarkers of systemic inflammation and risk of incident, symptomatic benign prostatic hyperplasia: results from the prostate cancer prevention trial. *Am. J. Epidemiol.*, **171**, 571–582.

28. Wang,W. *et al.* (2004) Chronic inflammation in benign prostate hyperplasia is associated with focal upregulation of cyclooxygenase-2, Bcl-2, and cell proliferation in the glandular epithelium. *Prostate*, **61**, 60–72.

29. Kaighn,M.E. *et al.* (1979) Establishment and characterization of a human prostatic carcinoma cell line (PC-3). *Invest. Urol.*, **17**, 16–23.

30. Halees,A.S. *et al.* (2003) PromoSer: a large-scale mammalian promoter and transcription start site identification service. *Nucleic Acids Res.*, **31**, 3554–3559.

31. Heinemeyer,T. *et al.* (1999) Expanding the TRANSFAC database towards an expert system of regulatory molecular mechanisms. *Nucleic Acids Res.*, **27**, 318–322.

32. Sboner,A. *et al.* (2010) Molecular sampling of prostate cancer: a dilemma for predicting disease progression. *BMC Med. Genomics*, **3**, 8.

33. Minn,A.J. *et al.* (2005) Genes that mediate breast cancer metastasis to lung. *Nature*, **436**, 518–524.

34. Aggarwal,B.B. *et al.* (2003) Anticancer potential of curcumin: preclinical and clinical studies. *Anticancer Res.*, **23**(1A), 363–398.

35. Pfeffer,U. *et al.* (2009) Prediction of breast cancer metastasis by genomic profiling: where do we stand? *Clin. Exp. Metastasis*, **26**, 547–558.

36. De Nunzio,C. *et al.* (2011) The controversial relationship between benign prostatic hyperplasia and prostate cancer: the role of inflammation. *Eur. Urol.*, **60**, 106–117.

37. Guess,H.A. (2001) Benign prostatic hyperplasia and prostate cancer. *Epidemiol. Rev.*, **23**, 152–158.

38. Lin,K., *et al.* (2008) Benefits and harms of prostate-specific antigen screening for prostate cancer: an evidence update for the U.S. Preventive Services Task Force. *Ann. Intern. Med.*, **149**, 192–199.

39. Chou,R., *et al.* (2011) Screening for prostate cancer: a review of the evidence for the U.S. Preventive Services Task Force. Dec 6;155(11):762-71. Epub 2011 Oct 7. *Ann Intern Med*.

40. Mukhopadhyay,A. *et al.* (2001) Curcumin downregulates cell survival mechanisms in human prostate cancer cell lines. *Oncogene*, **20**, 7597–7609.

41. Dorai,T. *et al.* (2000) Therapeutic potential of curcumin in human prostate cancer-I. curcumin induces apoptosis in both androgen-dependent and androgen-independent prostate cancer cells. *Prostate Cancer Prostatic Dis.*, **3**, 84–93.

42. Dorai,T. *et al.* (2001) Therapeutic potential of curcumin in human prostate cancer. III. Curcumin inhibits proliferation, induces apoptosis, and inhibits angiogenesis of LNCaP prostate cancer cells *in vivo*. *Prostate*, **47**, 293–303.

43. Khor,T.O. *et al.* (2006) Combined inhibitory effects of curcumin and phenethyl isothiocyanate on the growth of human PC-3 prostate xenografts in immunodeficient mice. *Cancer Res.*, **66**, 613–621.

44. Meigooni,D.S., *et al.* (2004) A novel method of enhancing prostate cancer radiosensitization by natural compound curcumin. *Med. Phys.*, **31**, 1733–1733.

45. Aggarwal,B.B. (2008) Prostate cancer and curcumin: add spice to your life. *Canc. Biol. Ther.*, **7**, 1438–1442.

46. Perkins,N.D. (2007) Integrating cell-signalling pathways with NF-kappaB and IKK function. *Nat. Rev. Mol. Cell Biol.*, **8**, 49–62.

47. Pahl,H.L. (1999) Activators and target genes of Rel/NF-kappaB transcription factors. *Oncogene*, **18**, 6853–6866.

48. Wilson,C. *et al.* (2008) Chemotherapy-induced CXC-chemokine/CXC-chemokine receptor signaling in metastatic prostate cancer cells confers resistance to oxaliplatin through potentiation of nuclear factor-kappaB transcription and evasion of apoptosis. *J. Pharmacol. Exp. Ther.*, **327**, 746–759.

49. Nannuru,K.C. *et al.* (2011) Role of chemokine receptor CXCR2 expression in mammary tumor growth, angiogenesis and metastasis. *J. Carcinog.*, **10**, 40.

50. Maxwell,P.J. *et al.* (2007) HIF-1 and NF-kappaB-mediated upregulation of CXCR1 and CXCR2 expression promotes cell survival in hypoxic prostate cancer cells. *Oncogene*, **26**, 7333–7345.

51. Goel,A. *et al.* (2010) Curcumin, the golden spice from Indian saffron, is a chemosensitizer and radiosensitizer for tumors and chemoprotector and radioprotector for normal organs. *Nutr. Cancer*, **62**, 919–930.

52. Kim,B.H. *et al.* (2011) Cyclooxygenase-2 overexpression in chronic inflammation associated with benign prostatic hyperplasia: is it related to apoptosis and angiogenesis of prostate cancer? *Korean J. Urol.*, **52**, 253–259.

53. Albini,A. *et al.* (2010) Functional genomics of endothelial cells treated with anti-angiogenic or angiopreventive drugs. *Clin. Exp. Metastasis*, **27**, 419–439.